PHYSICAL REVIEW D VOLUME 19, NUMBER 7 1 APRIL 1979

Connection between quark-model eigenstates and low-energy scattering

R. L. Jaffe and F. E. Low
Center for Theoretical Physics, Laboratory for Nuclear Science and Department of Physics, Massachusetts Institute of Technology, Cambridge, Massachusetts 02139
(Received 6 December 1978)

We propose a new method of analyzing low-energy hadron-hadron scattering designed to reveal internal quark-gluon eigenstates. Our method is a modification of the Wigner-Eisenbud formalism suited to the case of confining boundary conditions. We have identified a matrix function of the energy (which we call P) whose poles and residues correspond to the masses and channel projections of quark-gluon eigenstates calculated with spherical bag boundary conditions. To illustrate the formalism we apply it to the low-energy S-wave scattering of pseudoscalar mesons. We find from the data clear evidence of internal states corresponding to quark-model predictions of $Q^2\bar{Q}^2$ states at 0.69 and 1.04 GeV in the $I = 0$ channel, at 0.96 GeV in the $I = 1/2$ channel, at 1.19 GeV in the $I = 3/2$ channel, and at 1.04 GeV in the $I = 2$ channel. We believe the $I = 3/2$ and 2 internal states to be the low-energy exotics long predicted by quark models.

I. INTRODUCTION

In this paper we study the general relation between the discrete states that one would calculate in simple confined-quark models and low-energy hadron-hadron scattering. Our method of analyzing two-body reactions makes contact with bag-model calculations of both ordinary[1] ($Q\bar{Q}$ and Q^3) and multiquark[2] ($Q^m\bar{Q}^n$ with $n+m>3$) hadrons. We shall illustrate our discussion with the S-wave scattering of pseudoscalar mesons but our techniques apply also to higher partial waves and other two-body systems such as meson-nucleon and nucleon-nucleon.

We have identified a dynamical quantity—which we call the P matrix—which seves as a link between the discrete states of the quark model and the scattering states in which quarks do not appear. Quark-model eigenstates, suitably defined, correspond to poles in P with approximately calculable residues. The P matrix, in turn, is simple related to the S matrix and so may be extracted from measured phases and elasticities. Its poles may be compared with quark-model predictions. We find that the P-matrix description of S-wave meson-meson scattering is close to simple confined-quark-model expectations. Specifically, we find clear internal states (corresponding closely to the predictions of two-quark–two-antiquark bag calculations[2]) in the $I=0$, $\frac{1}{2}$, $\frac{3}{2}$, and 2 S-wave meson-meson channels, even though none of these "states" generates conventional resonant behavior in the phase shift.

The problem in identifying the discrete "states" of the bag model from scattering amplitudes is that these "states" are in general calculated with an artificial boundary condition which confines color-singlet as well as color-nonsinglet quark states. The "states" of Refs. 1 and 2 are in fact eigenstates of an approximate quark-gluon Hamiltonian which does not distinguish between colored and uncolored subunits. This is perhaps a realistic description of the $Q\bar{Q}$ and Q^3 systems, which possess only colored channels, but is not necessarily a good approximation for higher color-singlet configurations such as $Q^2\bar{Q}^2$ which must have unconfined color-singlet subunits.[3,4]

In the real world only the colored channels are confined. The color-singlet channels are unconfined and in fact constitute the objects in whose scattering we are interested. It can therefore happen that the discrete "states" are effectively created by the artificial barrier, in which case they may have a somewhat indirect relationship to the observed scattering, and the question of whether they should or should not be identified as "particles" in the Data Tables[5] becomes in the extreme cases a matter of taste. This does not mean that bag calculations of quark systems with color-singlet subunits are unpredictive. Quite the contrary, we find a reasonably precise although indirect relation between these discrete states and low-energy scattering. The discrete internal states are indeed present in the true scattering state in the sense that they provide a good approximation to the internal-region wave function over a significant energy range of the scattering.

This situation must be contrasted with the standard resonance physics in which there is a genuine physical barrier or weak coupling inhibiting the decay of the state. For example, the familiar, fairly narrow meson resonances presumably have their main components in the $Q\bar{Q}$ sector of the Hilbert space (where the confining barrier is real) and hence tend to be weakly coupled to the open

$Q\bar{Q}Q\bar{Q}$ channels. In addition, the decay of the lowest-lying unstable $Q\bar{Q}$ states is suppressed by an angular momentum barrier. Our description of low-energy scattering must (and will) reduce to this familiar picture for narrow states.

We have written "states" with quotes to emphasize the distinction between our objects and ordinary resonant states. To preserve the distinction it is convenient to give them a name of their own. Henceforth, we shall refer to eigenstates subject to perhaps artificial confining boundary conditions as *primitives*.

The connection between the primitives and the scattering can be illustrated in nonrelativistic potential theory. Consider a weak square-well potential of radius b and strength $V=-U/2m$. It is clear that there are no physical states or resonances created by this potential. However, if one imposes a boundary condition requiring the wavefunction to vanish at $r=b$ one creates an infinite set of internal states at

$$b(k_n^2+U)^{1/2}=n\pi, \quad n=1,2,\ldots . \tag{1.1}$$

Further, the phase shift $\delta(k)$ does nothing dramatic as k varies from 0 to ∞; it starts at zero, goes to an extremum $\delta_m=\pi/2-k_m b$ at

$$k_m b=[(\pi/2)^2-Ub^2]^{1/2} \tag{1.2}$$

and wiggles gently back to zero.[6] Nevertheless, we can precisely identify the primitives from the scattering by considering the quantity

$$P\equiv k\cot[kb+\delta(k)] \tag{1.3}$$

whose poles occur at the zero's of $\sin[kb+\delta(k)]$. Since $\sin[kb+\delta(k)]$ will have a zero when the true wave function vanishes at $r=b$, these zeros will precisely give us the roots k_n of Eq. (1.1). Indeed, for the square-well example, since

$$P=q\cot qb, \tag{1.4}$$

with

$$q=(k^2+U)^{1/2}, \tag{1.5}$$

we see that the poles of P are found at the zeros of $\sin qb$, or at $q_n b=n\pi$ in agreement with Eq. (1.1). Thus, the primitives calculated with the imposed boundary condition can be unambiguously identified with the poles of P. The primitives may be artificial, as in the case we have just considered. If, however, there is a physical boundary which genuinely confines the system, as in the case of the low-lying pseudoscalar and vector mesons where the major $Q\bar{Q}$ component of the wave function is confined by color, the primitives will correspond closely to conventional long-lived resonant states.

It is particularly instructive to pursue our square-well example to the extreme case of no interaction: $U=0$, $\delta(k)=0$. In that case

$$P=k\cot kb, \tag{1.6}$$

and the primitives—the poles in P—are at $k_n^2=n^2\pi^2/b^2$ with residues $2n^2\pi^2/b^3$. Now consider an arbitrary internal potential $V(r)$ which vanishes for $r>b$, and suppose it happened to generate a primitive at one of these momenta, say

$$k_1=\pi/b . \tag{1.7}$$

Then the scattering wave function at $k=k_1$ will be identical (for $r\geq b$) to the case of no interaction, and the phase shift, $\delta(k_1)$ will be zero. Furthermore, if the residue of the actual primitive is approximately $2\pi^2/b^3$, then the scattering wave function will resemble the noninteracting case for a wide range of k near k_1, and the primitive will have negligible impact on the scattering. We call this phenomenon "compensation" and refer to $E(k_1)=E_c$ as the "compensation energy." If the potential $V(r)$ generates a primitive at $E<E_c$ the primitive signals an attractive interaction and will show up as a positive phase shift. If the energy of the primitive is greater than E_c it signals repulsion and will show up as a negative phase shift. Of course, if the residue of the pole in P is small enough, indicating some physical barrier, there will be a nearby pole in the S matrix and a narrow peak in the cross section whatever the energy of the primitive. Otherwise the proximity of P-matrix poles to the compensation energy provides a useful qualitative measure of their effect on the phase shift.

One expects a continuum of situations ranging from "natural" confinement—such as the ρ, ϕ, and K^*—associated with truly resonant phase shifts, to "unnatural" confinement—such as the exotic $I=2$, 0^{++} primitive which we shall find at 1.04 GeV—associated with a slowly falling $\pi^+\pi^+$ phase shift (!), with intermediate cases—such as the $I=0$, 0^{++} primitive found at 0.69 GeV and the $S=1$, $I=\frac{1}{2}$, 0^{++} primitive found at 0.96 GeV—associated respectively with slowly rising $\pi\pi$ and πK phase shifts. All of these diverse effects, however, show up as clear poles in P.

In Sec. II we develop the formalism for translating information about the internal system into information about the scattering. In Sec. III we specialize to the bag model and techniques for casting its predictions into the form necessary for our analysis. In Sec. IV we apply our methods to the $I=0$, $\frac{1}{2}$, $\frac{3}{2}$, and 2 pseudoscalar meson-meson S-wave system in the GeV and sub-GeV region.

It is clear that if we really understood hadron dynamics this kind of analysis would be unneces-

sary. Thus, in our square-well example, there is no need to give special consideration to the poles of P; one could simply solve Eq. (1.2) for the phase shift $\delta(k)$. In the four-quark, meson-meson problem, however, we do not have a dynamical model that we can use to calculate the scattering directly from first principles. Therefore, we make a somewhat arbitrary division between an inside, within which we believe we can calculate quark-model primitives, and an outside, where the interaction between mesons is negligible, and attempt to join these regions by continuity. The joining process can then be used to construct the quantity analogous to P, Eq. (1.3), whose poles are the energy eigenvalues of the internal problem.

II. THE P MATRIX

We assume that outside a relative separation b in the center of mass the n-channel two-meson system is free and that continuum channels are unimportant. We may then choose n independent $l=0$ wave functions (see Appendix A for the derivation of P for higher partial waves):

$$\psi_{i,j}(r_j) \propto \delta_{ij}\cos k_j(r_j-b)+\frac{P_{ji}}{k_j}\sin k_j(r_j-b) \tag{2.1}$$

(where the first index on ψ labels the state, the second the channel) so that a pole of P corresponds to a state whose wave function vanishes at $r=b$, and hence to the kind of boundary condition on the internal wave functions which we wish to impose. We make contact with the S matrix by noting that

$$\psi_{i,j}(r_j)=\sum_l \frac{A_{li}}{\sqrt{k_j}}[\delta_{jl}\exp(-ik_jr_j)-S_{jl}\exp(ik_jr_j)] \tag{2.2}$$

for some matrix A. Solving for S,

$$S=-e^{-ikb}\frac{1-(i/\sqrt{k})P(1/\sqrt{k})}{1+(i/\sqrt{k})P(1/\sqrt{k})}e^{-ikb}. \tag{2.3}$$

In the one-channel case, of course, P reduces to $k\cot[kb+\delta(k)]$.

Note that $P=1/R$, where R is the matrix introduced by Wigner and Eisenbud. The extension of the Wigner-Eisenbud type formalism to particle reactions was proposed earlier by Breit and Bouricius and by Feshbach and Lomon.[7] The Feshbach-Lomon F matrix is essentially our P matrix, although the physics motivation is quite different. In the rest of this section, we give a list of useful formal properties of the P matrix. Many of these have already been discussed by Feshbach and Lomon, but we collect them here for convenience.

The matrix P has the following properties:

(a) It is real for real energies.

(b) It is symmetric.

(c) It has no two-body threshold singularities, and hence has only multiparticle and left-hand cuts, as well as essential singularities at ∞ introduced by the finite radius b. However, the importance of the finite plane singularities is expected to be drastically reduced compared to the case $b=0$. This is strongly suggested by our analysis of the left-hand cuts generated by potential scattering summarized in Appendix B. Potential scattering (e.g., a consequence of ρ, ω, σ exchange) occurs only for $r>b$, and is suppressed by a factor $e^{-Mb}\ll 1$, where M is the mass of the exchanged quantum. In nucleon-nucleon scattering pion exchange is important. We have estimated the effect of ρ exchange on $\pi\pi$ scattering and found it negligible.

(d) For a system satisfying a relativistic wave equation with a scalar potential, provided the interaction vanishes outside b, P can be expanded uniquely as a sum of poles with factorizing residues and a single matrix subtraction constant:

$$P_{ij}=C_{ij}+E^2\sum_n \frac{\lambda_i^n\lambda_j^n}{E^2-E_n{}^2}, \tag{2.4}$$

where $E^2=m^2+k^2$ and where the E_n are the eigenvalues of the internal Hamiltonian subject to the boundary condition $\psi=0$ at $r=b$. This is quite analogous to the case of the R matrix[7] where, however, no subtraction constant is required. Thus we expect P to be a slowly varying function of energy except for poles. In our square-well example Eq. (2.4) becomes the well-known expansion

$$x\cot x=1+2x^2\sum_{n=1}^{\infty}\frac{1}{x^2-n^2\pi^2}. \tag{2.5}$$

Of course, the interaction does not vanish exactly outside b, so that exchanges with range $1/M\gtrsim b$ must be taken into account as described in (c) above.

(e) P depends on b according to the equation

$$-\frac{dP}{db}=P^2+k^2, \tag{2.6}$$

so that a pole in $P\approx r(b)/[s-s_0(b)]$ at $s=s_0(b)$ has a residue which satisfies

$$\frac{-r(b)}{[s-s_0(b)]^2}\frac{\partial s_0}{\partial b}=\frac{r^2(b)}{[s-s_0(b)]^2} \tag{2.7}$$

or

$$r(b)=\left(-\frac{\partial s_0}{\partial b}\right)Q \tag{2.8}$$

with $Q^2=Q$. Here s is the usual channel invariant. Thus the residue of the pole is proportional to a projection operator which, in the absence of de-

generacy, will be given by a single vector ξ, that is,

$$Q_{ij} = \xi_i \xi_j \tag{2.9}$$

with $\sum_i \xi_1^2 = 1$.

This factorization can be seen directly. Consider $\tilde{S} = e^{ikb} S e^{ikb}$. This unitary matrix has eigenfunctions η^α with eigenvalues $e^{2i\bar{\delta}_\alpha}$. Hence

$$\tilde{S} = \sum_\alpha e^{2i\bar{\delta}_\alpha} |\eta^\alpha\rangle\langle\eta^\alpha| \tag{2.10}$$

and

$$P = \sum_\alpha \cot\bar{\delta}^\alpha \sqrt{k}\, |\eta^\alpha\rangle\langle\eta^\alpha| \sqrt{k}\,. \tag{2.11}$$

Barring accidental degeneracy, only one of the cotangents will have a pole, with residue given by Eq. (2.9) and

$$\xi_i^\alpha = \sqrt{k_i}\langle i|\eta^\alpha\rangle. \tag{2.12}$$

Note that the channel space, labeled by i, includes only physical, open scattering channels, not confined (e.g., $[(Q\bar{Q})^8 - (Q\bar{Q})^8]^1$) or closed channels.

(f) The effect on P of nearby closed channels is to produce an effective open channel P matrix $\tilde{P}$ given by

$$\tilde{P}_{oo} = P_{oo} - P_{oc} \frac{1}{P_{cc} + \kappa_{cc}} P_{co}\,, \tag{2.13}$$

where o and c represent open and closed channels, respectively. Here $\kappa_{cc} = -ik_{cc}$ and is real and positive. Thus, we shall see in Sec. IV, a pole in $\tilde{P}$ seen below the opening of a channel will be at a different energy from the true pole in P which can be observed above the channel threshold. This can be illustrated most clearly by specializing Eq. (2.13) to the case of a single factorizable pole in P at s_0, plus a background that is diagonal in the closed channel:

$$P_{ij} = a_{ij} + \frac{\lambda_i \lambda_j}{s - s_0}, \tag{2.14}$$

where $a_{cc'} = a_c \delta_{cc'}$. The closed-channel P matrix is then

$$P_{cc} = a_c \delta_{cc'} + \frac{\lambda_c \lambda_{c'}}{s - s_0}\,. \tag{2.15}$$

The closed-channel inverse of $P + \kappa$ is easily calculated and substituted into Eq. (2.13). We find

$$\tilde{P}_{ij} = a_{ij} - \sum_c \frac{a_{ic} a_{jc}}{d_c} + \frac{(\lambda_i - \sum_c a_{ci}\lambda_c/d_c)(\lambda_j - \sum_c a_{cj}\lambda_c)}{s - s_0 + \sum_c \lambda_c^2/d_c}, \tag{2.16}$$

where $d_c = a_{cc} + \kappa_{cc}$ and i and j represent open channels. Thus, the original pole has disappeared, and a displaced pole with a modified residue has appeared in its place.

Finally, we note that the only theoretical limitation on the range of application of this formalism is its inability to parametrize multibody channels. In meson-meson scattering multibody channels do not appear to become important until energies in excess of 1.5 GeV. Practical application of our formalism is handicapped by lack of good data, profusion of two-body channels and the large number of P-matrix poles expected in quark models well before this theoretical limit.

III. CONNECTION TO THE BAG MODEL

One approach would be to view the matching radius, b, as a parameter and to extract the P matrix from low-energy scattering data for arbitrary b (providing b is outside the interaction region). However, we wish to make contact with confined-quark-model calculations which can predict the values of s_0, b, and the projection operator $\xi_i \xi_j$. We shall relate $\sqrt{s_0}$ to the mass of the primitive as calculated in the bag model, b to its radius, and ξ_i to its components on channel wave functions (e.g., $\pi\pi$, $\eta\eta$, $K\bar{K}$, etc.). The data also determine the residue $-ds_0/db$ which we can relate only qualitatively to bag-model calculations.

We make the connection firstly by assuming that a primitive of the spherical bag model with radius R corresponds to a pole in the P matrix, $P(b)$, with $b = b(R)$. By this we imply (a) that the bag boundary condition on a quark state—which says that hadronic matter ends at R—is to be understood to require the vanishing of the meson-meson wave functions at some relative separation $b(R)$; and (b) that there is no significant interaction between color-singlet meson constituents outside the radius b. To estimate the relation between b and R, consider the four-quark density function $\rho(\vec{r}_1, \vec{r}_2, \vec{r}_3, \vec{r}_4)$ inside a spherical $Q^2\bar{Q}^2$ bag. $\rho(\vec{r}_1, \vec{r}_2, \vec{r}_3, \vec{r}_4)$ is different from zero only inside the bag. Therefore, the effective two-body density,

$$\rho(\vec{r}, \vec{r}_c) = \int d^3r_1 d^3r_2 d^3r_3 d^3r_4 \delta^3\left(\frac{\vec{r}_1 + \vec{r}_2}{2} - \frac{\vec{r}_3 + \vec{r}_4}{2} - \vec{r}\right) \times \delta\left(\frac{\vec{r}_1 + \vec{r}_2 + \vec{r}_3 + \vec{r}_4}{4} - \vec{r}_c\right) \rho(\vec{r}_1, \vec{r}_2, \vec{r}_3, \vec{r}_4)\,, \tag{3.1}$$

will vanish strongly as the relative separation r approaches twice the bag radius, $2R$.[8] This may be seen in Fig. 1(a), where we have plotted $\rho(r) \equiv \int d^3r_c \rho(\vec{r}, \vec{r}_c)$ for the lowest S-wave bag wave function. We associate the strong vanishing of $\rho(r)$ at $2R$ with the P-matrix boundary condition

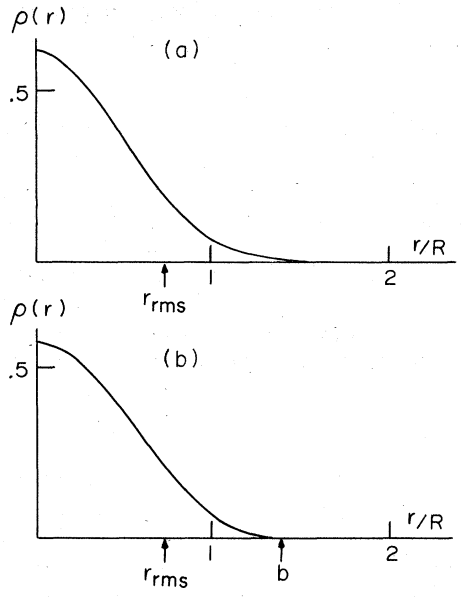

FIG. 1. (a) The density for the meson-meson separation in the ground-state spherical $Q^2\bar{Q}^2$ bag (Ref. 18). (b) The density for a free meson-meson wave function with its first zero at $r=b$. b is chosen so that the rms radius of this wave function matches the rms radius in Fig. 1(a).

at b. We estimate the matching radius $b(R)$ by equating the mean value of $\vec{r}^2$ obtained from Eq. (3.1) and the S-wave functions:

$$\langle r^2\rangle = \int d^3r_1 d^3r_2 d^3r_3 d^3r_4 \left(\frac{\vec{r}_1+\vec{r}_2}{2}-\frac{\vec{r}_3+\vec{r}_4}{2}\right)^2 \times \rho(\vec{r}_1,\vec{r}_2,\vec{r}_3,\vec{r}_4) = \langle r_1^2\rangle , \tag{3.2}$$

where

$$\langle r_1^2\rangle = \int d^3r\, r^2 |\psi_q(r)|^2 \tag{3.3}$$

[where $\psi_q(r)$ is the lowest S-wave bag eigenstate wave function] with the mean value of r^2 obtained from a free meson-meson wave function $\psi(r)$ which vanishes at $r=b$, i.e.,

$$\psi(r) = \frac{1}{(2\pi b)^{1/2}} \frac{\sin\pi r/b}{r} . \tag{3.4}$$

The resulting relationship is

$$b \simeq 1.4R . \tag{3.5}$$

This procedure is displayed graphically in Fig. 1(b).

We expect the energy of the P-matrix pole in question to be closest to that of the calculated bag primitive when Eq. (3.5) is used to determine b.

A bag-model virial theorem relates R to the mass (M) of the primitive:

$$R = \left(\frac{3M}{1b\pi B}\right)^{1/3} = 5M^{1/3}\ \mathrm{GeV}^{-1} \tag{3.6}$$

for M in GeV. Equation (3.6) holds exactly only for massless (u and d) quark systems but is approximately valid for systems containing strange quarks. Combining Eqs. (3.5) and (3.6) we obtain

$$b = b(M) = 7M^{1/3}\ \mathrm{GeV}^{-1} \tag{3.7}$$

for M in GeV.

To proceed further and predict ξ_i and ds_0/ab, we must make a more detailed model for the channel couplings of the bag states. The $Q^2\bar{Q}^2$ primitives of Ref. 2 were given there in a $Q\bar{Q}$-$Q\bar{Q}$ basis. The $Q\bar{Q}$ subunits are color singlets or octets with the flavor and spin quantum numbers of the familiar pseudoscalar and vector mesons. For example, the lowest-mass $Q^2\bar{Q}^2$ primitive, a scalar isosinglet at 650 MeV, is written as[10]

$$\begin{aligned}|C^0(9)0^{++}\rangle = {} & 0.64|\pi\pi\rangle - 0.37|\vec{\pi}\cdot\vec{\pi}\rangle + 0.19|\eta\eta\rangle \\ & - 0.11|\vec{\eta}\cdot\vec{\eta}\rangle + 0.29|\rho\rho\rangle - 0.34|\vec{\rho}\cdot\vec{\rho}\rangle \\ & + 0.16|\omega\omega\rangle - 0.20|\vec{\omega}\cdot\vec{\omega}\rangle + \cdots .\end{aligned} \tag{3.8}$$

One is tempted to identify the components of the $Q^2\bar{Q}^2$ primitive in this basis as the components of the vector ξ_i. But this is wrong, since ξ_i cannot have components in confined channels. Our formalism requires no significant interaction for $r>b$. Therefore, the channel space of ξ_i can contain only physical open scattering channels.

To identify ξ_i imagine carrying out a static bag calculation for various radii. For small radius confining forces are unimportant, quantum chromodynamics (QCD) does not appear to distinguish between uncolored and colored subunits, and quark kinetic energies dominate. As the radius increases, confining forces become more important—represented by the bag energy BV. For systems *with no* color-singlet subunits (e.g., $Q\bar{Q}$) an equilibrium radius, R, is fixed by the balance of quark kinetic and bag energies. For systems with color-singlet subunits, the spherical-cavity approximation breaks down. It predicts an equilibrium radius in this case also, whereas we expect that the physical system can continue to lower its energy by expanding into the unconfined channels. We will assume that the confining forces are such that the confined components of the primitive disappear by a radius R' only slightly greater that the static cavity equilibrium radius R, and that the relative strengths of the various *unconfined*-channel couplings do not change significantly between R and R'. We assume the same to be true

of ordinary closed channels. Thus, for the bag primitive at 650 MeV described by Eq. (3.8), we treat the $\rho\rho$ channel, which is 1 GeV closed, the same as the $\vec{p}\cdot\vec{p}$ channel which is permanently closed, i.e., confined. We estimate then that the unit vector ξ_i is given by

$$\xi_o = \frac{\zeta_o}{(1-\sum_c \zeta_c^2)^{1/2}}, \tag{3.9}$$

where $\{\zeta_i\}$ are the coefficients in the static cavity wave functions as in Eq. (3.8), and the subscripts denote open (o) and confined or closed (c) channels. Our example of Eq. (3.8), the 650-MeV isosinglet, becomes trivial. Only the $\pi\pi$ channel is open, so $\xi_{\pi\pi}=1$. For systems with more than one open channel, the results are not trivial. This prescription is clearly a crude approximation. To improve upon it one must study the dynamics of bag deformation and fission, perhaps in the manner already suggested by DeTar (see Ref. 4).

In order to estimate the slope ds_0/db, and hence the residue of the P-matrix pole, we assume that the spherical-cavity bag approximation is a good one for sufficiently small b. The successful bag-model phenomenology of the conventional two- and three-quark hadron states makes this a reasonable starting point, since we do not expect the separation of color-singlet components to be significant until these components can themselves fit comfortably into the allowed volume. As we increase the constraining radius, the true four-quark system will begin to expand into its open channels. We attempt to take this into account by removing the bag pressure in the open channels. Thus, the Hamiltonian of the system, constrainted to the radius R, is chosen to be

$$H = H_B(R) - \Lambda \tfrac{4}{3}\pi B R^3, \tag{3.10}$$

where $H_B(R)$ is the Hamiltonian of the spherical bag approximation for the four-quark system, and Λ is the projection onto the open channels. B is the bag constant, $B^{1/4}=145$ MeV. Our previous calculation of the location of "primitives" chose R at the minimum of $H_B(R)$; therefore, the derivative, ds_0/db, is completely given by the second term in (3.10)

$$-\frac{dE_0}{db} = \langle\Lambda\rangle 4\pi B R^2 \frac{dR}{db} \tag{3.11}$$

or

$$-\frac{1}{E_0}\frac{dE_0}{db} = \frac{3}{4}\langle\Lambda\rangle \frac{1}{R}\frac{dR}{db} \tag{3.12}$$

by the virial theorem, so that

$$-\frac{1}{s_0}\frac{ds_0}{db} = \frac{3}{2}\frac{\langle\Lambda\rangle}{b}. \tag{3.13}$$

It must finally be the case that b is large enough so that the component particles are substantially free for $r>b$, since otherwise our analysis connecting the P matrix to the S matrix will not be valid. A first criterion is that the volume of the system be larger than the volume of its separated components. Since the volume is proportional to the mass, this criterion is equivalent to demanding that the mass of the primitive be larger than the masses of the components. This is modestly satisfied for the two-pion system in our calculations, but not at all for the $K\bar{K}$ system. Hence, we should be more suspicious of the residue calculation in that problem than we are in the two-pion system. A second criterion can be obtained by explicit calculations of the effect of final-state interactions on our analysis. As noted in the previous section, we have carried out such calculations for ρ exchange in the π-π system and found only very small corrections (see Appendix B).

The projection onto open channels is determined by the coefficients $\{\zeta_i\}$ in the bag wave functions such as Eq. (3.8). Thus,

$$\langle\Lambda\rangle = \sum_o \zeta_o^2, \tag{3.14}$$

where (o) denotes open channels and the sum over all channels $\sum_i \zeta_i^2$ is unity. Thus, for example, we predict $\langle\Lambda\rangle = (0.64)^2$ for the 650-MeV scalar isosinglet.

We must reemphasize the crudity of this model for the residues. We have assumed that inside b the system can be described by the spherically symmetric bag, that outside b it can be described by the noninteracting particles, and that for r near b the transition may be described by simply turning off the bag pressure in the open channels. If all this came within 50% of the correct residues of the P-matrix poles we would be delighted.

At the same time, we also reemphasize the general validity of our discussion of P-matrix poles, and of the approximate calculation of their location by the spherical bag model. A possible estimate of accuracy is given by the correction to the Hamiltonian in Eq. (1):

$$\delta E = -\tfrac{1}{4}\langle\Lambda\rangle E \sim -\tfrac{1}{8}E. \tag{3.15}$$

Thus, we expect the location of primitives to be within 10–20% of the original calculation, and generally somewhat lower.

IV. P-MATRIX ANALYSIS OF LOW-ENERGY S-WAVE MESON-MESON SCATTERING

To illustrate the formalism of the preceding sections we shall study the S-wave pseudoscalar meson-meson P matrix at low energies. The 0^{++}

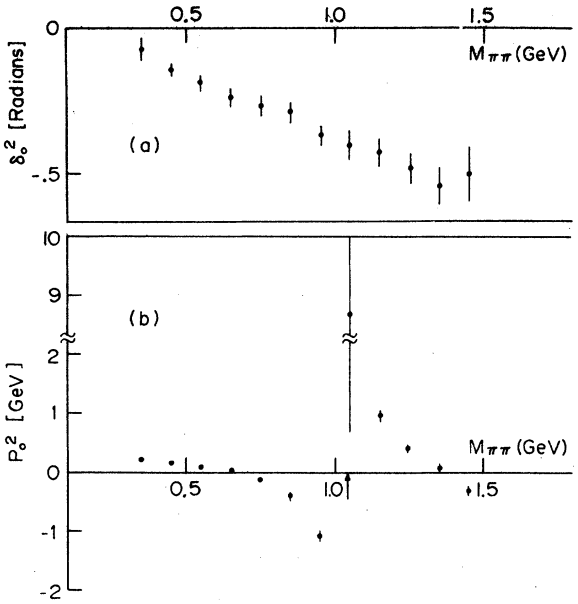

FIG. 2. (a) $\pi\pi$ $I=2$ (exotic) S-wave phase shift (Ref. 19). (b) $\pi\pi$ $I=2$ S-wave P-matrix element. The arrow marks the P-matrix pole.

channels have been the source of some confusion in recent years. The data show a variety of enhancements, few of which are clearly resonant. Bag calculations lead us to expect $Q^2\bar{Q}^2$ configura-

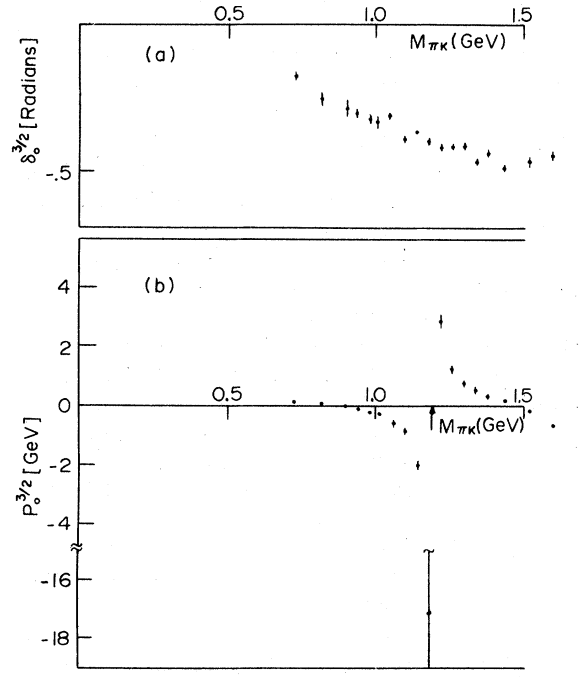

FIG. 3. (a) πK $I=\frac{3}{2}$ (exotic) S-wave phase shift (Ref. 20). (b) πK $I=\frac{3}{2}$ S-wave P-matrix element. The arrow marks the P-matrix pole.

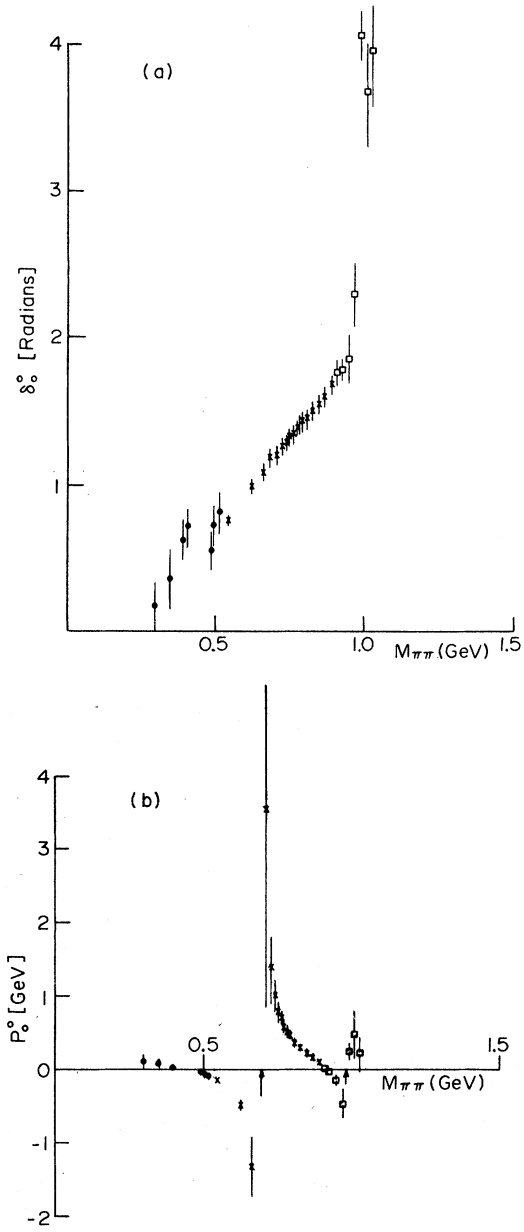

FIG. 4. (a) $\pi\pi$ $I=0$ (nonexotic) S-wave phase shift for $\sqrt{s} \lesssim 2M_K$. Crosses are from Ref. 21; open boxes from Ref. 13 and solid boxes from several sources quoted in Ref. 5. (b) $\pi\pi$ $I=0$ (nonexotic) S-wave P-matrix element for $\sqrt{s} \lesssim 2M_K$. The arrows mark the P-matrix poles.

tions to be important at low mass and to obscure the usual $Q\bar{Q}$ resonances. We believe these complexities can be sorted out (at least at low energies) by constructing the P matrix and studying its singularities.

Sufficient data exist for us to construct the P matrix for the $I=0$, $\frac{1}{2}$, $\frac{3}{2}$, and $2\ 0^{++}$ channels over a range of energies. The absence of any phase-

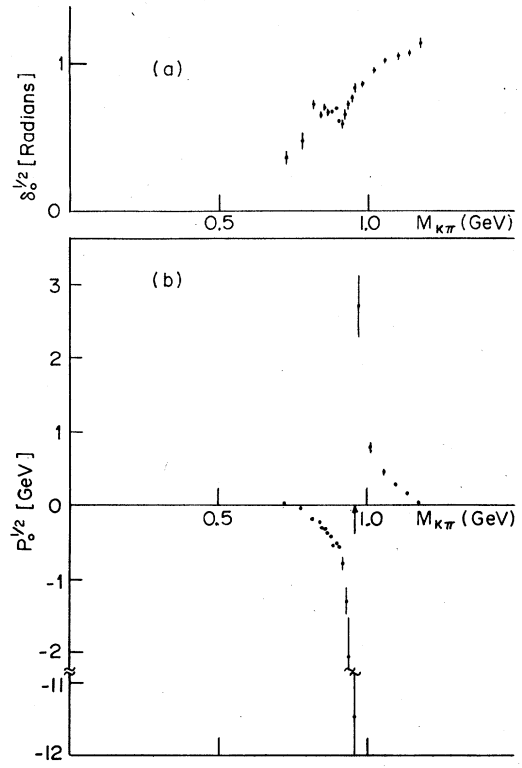

FIG. 5. (a) πK $I=\frac{1}{2}$ (nonexotic) S-wave phase shift (Ref. 19). (b) πK $I=\frac{1}{2}$ (nonexotic) S-wave P-matrix element. The arrow marks the P-matrix poles.

shift analysis of $\pi\eta \to \pi\eta$ precludes a similar treatment of the $I=1$ channel. When only one channel is open, P may be constructed from Eq. (1.3). When several channels are open, the analysis is more complicated. Below we will illustrate the two-channel problem in the $I=0$ $\pi\pi$ and $K\bar{K}$ channels.

TABLE I. P-matrix poles found in the analysis of single-channel S-wave meson-meson scattering data.

Channel[a]	Pole location (GeV)	Residue (GeV^3)
$\pi\pi^0$	0.69	0.064
	0.98	0.009
$\pi K^{1/2}$	0.96	0.079
$\pi\pi^2$	1.04	0.21
$\pi K^{3/2}$	1.19	0.22

[a] We use the notation MM^I to distinguish between possible total isospins.

First, let us study the one-channel systems. The phase shifts $\delta_0^I(k)$ and the associated $P_0^I(k)$ are shown in Figs. 2–5. Our analysis is not sensitive to the exact value of the matching radius b or its functional dependence on M within wide limits. We will discuss the important of b in more detail below. In Figs. 2–5, we used the bag-model estimate for $b=b(M)$ given in Eq. (3.7). The striking features of Figs. 2–5 are the clear poles in P in *all* channels. The pole locations and residues are summarized in Table I.[11]

The bag model predicts primitives in all these channels. For an immediate comparison with Table I we record in Table II the masses and residues of the lightest bag primitives in the 0^{++} channels obtained from Ref. 2 (see especially Table IV and Fig. 6) and Eqs. (2.8), (2.9), (3.13), and (3.14). These are all $Q^2\bar{Q}^2$ configurations. The $Q\bar{Q}$-0^{++} primitives are heavier and outside the region we have analyzed, with the exception of the $\pi\pi^0$ channel at energies greater than 1 GeV. Their possible importance in this channel is discussed below.

Rather than discuss these results channel by

TABLE II. Predicted masses and residues of the lightest bag-model 0^{++} primitives.

Name[a]	J^PI^G	Channels[b]	Predicted mass (GeV)	Predicted residue[c] (GeV^3)
$C^0(9)$	0^+0^+	$\pi\pi^0, K\bar{K}^0, \eta\eta$	0.65	0.04
$C^s(9)$	0^+0^+	$K\bar{K}^0, (\pi\pi^0)^d, \eta\eta$	1.10	0.07[e]
$C_K(9)$	$0^+\frac{1}{2}$	$\pi K^{1/2}, \eta K$	0.90	0.07
$C_\pi^s(9)$	0^+1^-	$K\bar{K}^1, \pi\eta$	1.10	0.10
$E_{\pi\pi}(36)$	0^+2^+	$\pi\pi^2$	1.15	0.11
$E_{\pi K}(36)$	$0^+\frac{3}{2}$	$\pi K^{3/2}$	1.35	0.15
$E_{KK}(36)$	0^+1	KK^1	1.55	0.19

[a] See Ref. 2.

[b] The open channel(s) in which the pole is expected to be seen is (are) underlined. Only pseudoscalar-meson channels are listed.

[c] $-ds_0/db$. See Eq. (2.8).

[d] The coupling of this state to $\pi\pi$ is forbidden in the OZI limit.

[e] The residue is calculated assuming $K\bar{K}^0$ and $\pi\pi^0$ are the open channels, and is not to be compared with the single-channel residue of Table I.

channel we prefer to make a series of general comments illustrated by reference to specific channels. First, we discuss exotics and suggest a solution to the long-standing exotics problem in the quark model. Then we turn to the nonexotic channels. In addition to the results presented in Tables I and II we analyze the two-channel $\pi\pi$ and $K\bar{K}$ isosinglet S wave near and slightly above $K\bar{K}$ threshold. We discuss the implications of our analysis for the so-called scalar mesons. Thirdly, we construct the P matrix for the $\pi\pi$ P wave at low energy in order to show that we obtain a satisfactory description of familiar resonances such as the ρ meson. Finally, we discuss the dependence of our results on the prescription for the matching radius $b(M)$.

A. Exotics

We have found a resolution of the exotics problem in the bag model:

(a) The usual bag calculations predict exotic "states" at low energies in $\pi\pi$ and πK channels (see Table II).

(b) The data show no exotic resonances at low energies.

(c) Facts (a) and (b) are consistent. In fact, the falling phase shifts in exotic channels require P-matrix poles at masses very close to those predicted by the bag model.

Exotic channels are the cleanest from our standpoint. Ignoring continuum multimeson production the exotic channels are one-channel systems until well above 1.5 GeV (until $\rho\rho$, ρK^* and K^*K^* thresholds). There are no $Q\bar{Q}$ primitives and only two predicted $Q^2\bar{Q}^2$ primitives in each channel[2]—the one listed in Table II and another about 0.65 GeV heavier. Therefore, a simple pole approximation to the P matrix is expected to be valid over a wide range of energies.

In the bag model, exotic primitives are made heavier by color magnetic interactions. This is at the root of the negative phase shifts seen in exotic channels. The connection is obvious when the compensation energies for the exotic channels are calculated. Using $k_1 = \pi/b(M)$ with $b(M)$ given by Eq. (3.8), we find compensation energies of $E_c(\pi\pi) = 0.95$ and $E_c(\pi K) = 1.08$ for $\pi\pi$ and πK, respectively. In each exotic channel the bag-model primitive is heavier than the compensation energy; it therefore signals repulsion (see Sec. I) and a negative phase shift. In other words the negative phase shifts of Figs. 2 and 3 are *direct experimental evidence for the repulsive color-magnetic interactions predicted in exotic channels by QCD.*

The predicted residues are too small. The projection onto open channels, $\langle\Lambda\rangle$, which figures into the residue via Eq. (3.13) is 0.41 for the spherical exotics of Ref. 2. To obtain agreement with experiment, $\langle\Lambda\rangle \sim 1$ is required. Apparently, the physical primitives are even more strongly coupled to the open channels than the model of Sec. III led us to suspect. This should not be surprising. Our model is very crude—in particular, it treats all channels equivalently at the equilibrium bag radius R. Consider, for example, the $I = 2$ channel. Since the pion is very light we would expect correlations which make the primitive look more like two pions to be energetically favored. However, the simple model of Sec. III places all quarks in the S wave and consequently forbids correlations in which pionlike lumps separate. We therefore expect the physical primitive to be less massive and more strongly coupled to $\pi\pi$ than S-wave spherical primitives.

B. Nonexotic channels

Both the $\pi\pi^0$ and $\pi K^{1/2}$ phase shifts show broad enhancements in the 500 MeV above threshold. The resonant nature of these bumps have been debated for many years. These attractive phase shifts result in P-matrix poles at 0.69 and 0.96 GeV, respectively. As before, the behavior of the physical phase shift can be understood by comparing the location of the P-matrix pole with the compensation energy, E_c. Because of attractive color-magnetic forces the $\pi\pi^0$ and $\pi K^{1/2}$ primitives are both lighter than the relevant compensation energies—hence, the positive phase shifts in these channels. Once again low-energy S-wave meson-meson scattering provides experimental evidence for color magnetic forces, this time in attractive, cryptoexotic configurations.

Sufficient data exist to perform a two-channel analysis of the isosinglet $\pi\pi$-$K\bar{K}$ system up to $\eta\eta$ threshold (1100 MeV). This is of more than academic interest because of the presence of a narrow effect very close to $K\bar{K}$ threshold—the so called S^* meson. We see the S^* in two different ways: First, in Fig. 4 we see a narrow pole in the $\pi\pi^0$ P matrix right at $K\bar{K}$ threshold. Its mass is 0.98 GeV and its residue is 0.009 GeV^3, nearly an order of magnitude less than the lower pole in the same channel. Because of the proximity of $K\bar{K}$ threshold, this must be regarded as a pole in the *reduced* P matrix, as discussed in Sec. II(f). Its residue is not indicative of the true P-matrix pole, but instead is given by Eq. (2.16). Second, we expect to see a pole in the full two channel P matrix at a mass greater than 0.98 GeV.

The two-channel P matrix can be extracted from the two-channel partial-wave S matrix

$$S=\begin{pmatrix} \eta e^{2i\delta_1} & i(1-\eta^2)^{1/2}e^{i(\delta_1+\delta_2)} \\ i(1-\eta^2)^{1/2}e^{i(\delta_1+\delta_2)} & \eta e^{2i\delta_2} \end{pmatrix}$$

where δ_1 is the phase of $\pi\pi\to\pi\pi$, and δ_2 is the phase of $K\bar{K}\to K\bar{K}$:

$$P_{11}=\frac{k_1}{D}[\eta\sin(\theta_1-\theta_2)-\sin(\theta_1+\theta_2)]\equiv N_{11}/D\,, \quad (4.2)$$

$$P_{12}=P_{21}=\frac{(k_1k_2)^{1/2}}{D}(1-\eta^2)^{1/2}\equiv N_{12}/D\,, \quad (4.3)$$

$$P_{22}=-\frac{k_2}{D}[\eta\sin(\theta_1-\theta_2)+\sin(\theta_1+\theta_2)]\equiv N_{22}/D\,, \quad (4.4)$$

with

$$D=\cos(\theta_1+\theta_2)-\eta\cos(\theta_1-\theta_2) \quad (4.5)$$

and

$$\theta_i=k_ib+\delta_i\,. \quad (4.6)$$

Although it is not obvious, P_{ij} has no threshold singularities as $k_2\to 0$. This provides an explicit example of the general result quoted in Sec. II. Because of this it should be possible to separate out the underlying S^* effect from the complexities introduced by the proximity of $K\bar{K}$ threshold. In principle, one should (a) construct the full two-channel P matrix; (b) locate the pole if there is one, (c) parametrize it according to Eq. (2.14). Then (d) construct the reduced P matrix according to Eq. (2.16) which finally should account for the narrow S^* effect seen in the $\pi\pi$ channel below $K\bar{K}$ threshold.

Available data are not precise enough for us to carry this through completely. We are able to construct the full P matrix and find the S^* pole, but we can only crudely complete steps (c) and (d). Phase shifts from the most recent high-statistics measurements[12] of $\pi\pi$ scattering have not been published. We have used older[13] and lower-statistics[14] data. Measurements of the $K\bar{K}$ phase are very difficult. We have used an analysis by Estabrook giving $\delta_1+\delta_2$ above 1 GeV.[15] The resulting P-matrix elements are shown in Fig. 6. Because the errors are large, we have plotted the numerators of Eqs. (4.2)–(4.4) separately from the common denominator D. We see fairly convincing evidence for a pole in P (a zero in D):

$$P_{ij}=\frac{r\xi_i\xi_j}{s-s_0}$$

at $\sqrt{s_0}\sim 1.04$ GeV with a residue $r\sim 0.10$ and couplings $\xi_{\pi\pi}\sim 0.8$ and $\xi_{K\bar{K}}\sim 0.6$.

Apparently, the true P-matrix pole corresponding to the S^* has a residue comparable to the resi-

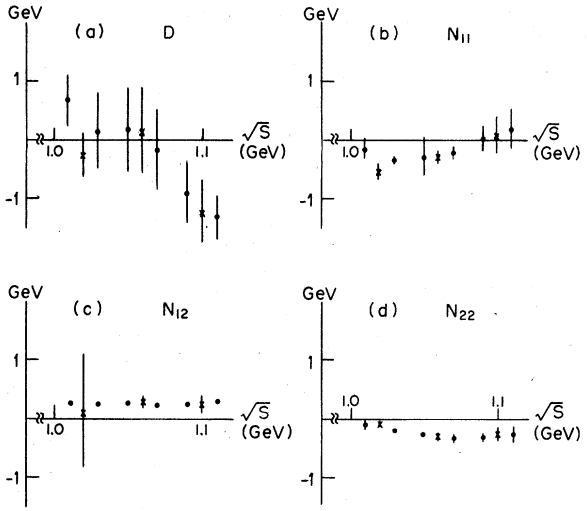

FIG. 6. P-matrix elements for $\pi\pi$ and $K\bar{K}$ $I=0$ S wave for $1.01<\sqrt{s}<1.11$ GeV. $\pi\pi$ data were taken from Refs. 13 (solid circles) and 14 (crosses), $K\bar{K}$ data came from Ref. 15. Reference 13 did not assign errors to the elasticity η. We assumed (somewhat unrealistically) no error in η. For notation see Eqs. (4.2)–(4.5).

dues of the other low-mass nonexotic primitives (see Table I), not withstanding the fact that the reduced P-matrix pole is very narrow. This shift must be a consequence of the reduction procedure which also shifts the pole from ~1.04 GeV down to ~0.98 GeV. To find these pole and residue shifts we require the constants a_{KK} and $a_{\pi K}$ in addition to the vector $(\xi_{\pi\pi}, \xi_{K\bar{K}})$ already quoted. a_{KK} and $a_{\pi K}$ depend on the slopes of the functions N_{12} and N_{22} which are not well determined by the data. It is also necessary to know the curvature in D near its zero, which we cannot reliably estimate from Fig. 6. So the crude data vaailable to us are not sufficient to extrapolate P below $K\bar{K}$ threshold and look for the pole in $\bar{P}$.[16] The ratio of the S^* (the 1.04-GeV primitive) coupling to $\pi\pi$ and to $K\bar{K}$ presents a problem. The bag primitive predicted at 1.1 GeV has quark content $s\bar{s}(u\bar{u}+d\bar{d})$ and should not couple to $\pi\pi$ in the Okubo-Zweig-Iizuka (OZI) limit. We know of at least three mechanisms which could generate this coupling for the $S^*(1.04)$, but not effect our other results. First, the bag primitive does couple to $\eta\eta$ and that threshold is nearby. According to Eq. (2.16) a nearby closed channel can generate a new coupling in the reduced P matrix. Second, the $Q\bar{Q}$ 0^{++} primitives are expected at energies in this range. Mixing of these nearby primitives may generate large OZI-rule violations. Finally, there are other $Q^2\bar{Q}^2$ primitives—brothers of the exotic $E_{\pi\pi}(36)$—predicted in this energy range[2] with which the S^* may mix. Clearly the $I=0$ $\pi\pi$, $K\bar{K}$,

$\eta\eta$ system deserves further experimental and theoretical study.

To summarize we have found clear evidence for three nonexotic scalar-meson primitives, two in the isoscalar channel and the third with $I=\frac{1}{2}$ and strangeness ± 1. The masses of these primitives correspond closely to the masses expected of the $Q^2\bar{Q}^2$ nonet as discussed in Ref. 2. The remaining member of the nonet is the $I=1$ nonstrange object expected in the $K\bar{K}$ and $\pi\eta$ channels. We know of no measurements of $\pi\eta \to \pi\eta$ so we cannot construct the P matrix in this channel. However, we expect that the fairly narrow enhancement seen in the $\pi\eta$ mass spectrum and known as the $\delta(970)$ will complete the nonet. Very likely the situation is similar to the $I=0$ channel: The P matrix has a pole above $K\bar{K}$ threshold which is reflected in a narrower pole in the $\pi\eta$-reduced P matrix below $K\bar{K}$ threshold.

Of course, an entire extra nonet of scalar mesons from the $Q\bar{Q}$ configuration is expected at energies in excess of 1 GeV. These must show up as P-matrix poles and, if narrow, may resonate. There is already evidence for these states [$\epsilon'(1300)$, $\delta'(1300)$, $\kappa(1450)$] as summarized by Martin.[17] As already mentioned, we expect mixing between the heavier $Q^2\bar{Q}^2$ and lightest $Q\bar{Q}$ primitives.

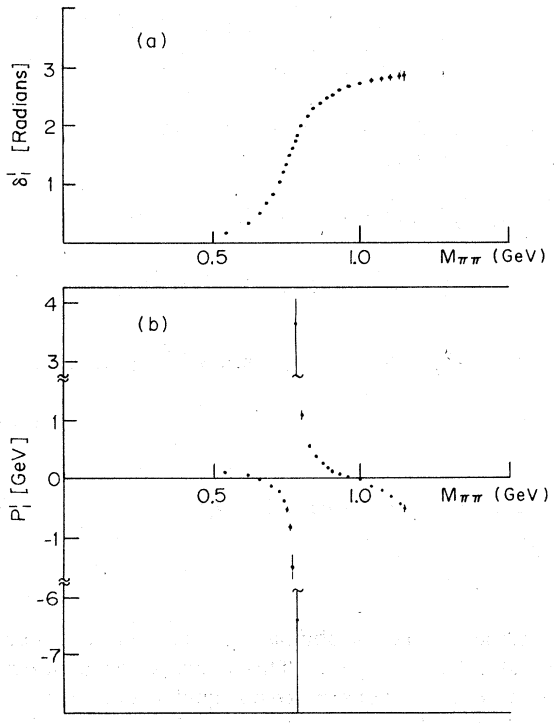

FIG. 7. (a) $\pi\pi$ $I=1$ P-wave phase shift showing the ρ-meson resonance (Ref. 21). (b) $\pi\pi$ $I=1$ P-wave P-matrix element showing the ρ pole.

C. The ρ meson

The $\pi\pi$ P-wave phase shift is plotted in Fig. 7(a). In Appendix A we show how to construct the P matrix for arbitrary partial waves. From Eq. (A8) we extract the $\pi\pi$ P-wave P matrix which is plotted in Fig. 7(b). As promised the rapid variation in the phase generates a nearby pole in P. Though the phase goes through $\pi/2$ near 770 MeV the P-matrix pole is at 788 MeV. The difference may be regarded as the relaxation of the primitive into the open $\pi\pi$ channel. Notice that it is the primitive mass, not the mass quoted in the Data Tables, which should be compared with quark-model calculations, e.g., in calculations of ρ-ω mixing. The residue of the ρ-meson P-matrix pole is 0.03 GeV^3. From Eq. (3.13) we obtain the projection onto open channels of $\langle\Lambda\rangle=(\zeta_{\pi\pi})^2=0.23$. For comparison the S-wave $\pi\pi$ P-matrix pole at 0.69 GeV has a residue of 0.06 corresponding to $\zeta_{\pi\pi}{}^2=0.52$. The ρ is half as strongly coupled to the open channel. Note, however, that even if $(\zeta_{\pi\pi})^2$ for the ρ were as large as 0.5, the ρ would still show up as a "resonance": (a) because the pole location (788 MeV) is so far below the P-wave compensation energy ($k_1=4.49/b=0.60$ GeV so $E_c=1.23$ GeV) signalling strong attraction, and (b) because the angular momentum barrier [reflected in the kinematic factors of Eq. (A8)] makes the effect narrow. A P-matrix study of familiar resonances will provide input to calculations of configuration mixing $(Q\bar{Q}+Q^2\bar{Q}^2+\cdots)$ in quark models.

D. b-dependence

We have chosen to analyze the meson-meson S wave with the simple form $b=7M^{1/3}$ GeV^{-1}. A different choice would shift the locations but within the wide limits not change the qualitative results. The shift in s_0 with b is given by $\partial s_0/\partial b$ which also measures the residue of the pole. Thus narrow objects like the ρ meson or even better, ϕ meson, are not b-dependent. This is reasonable: as we have emphasized, objects are narrow because of real, physical barriers such as confinement. Moving the artificial barrier has little effect on the primitive when b is outside the physical barrier. Figure 8(a) shows the dependence of the location of the ρ-meson P-matrix pole on b. It requires an unreasonable choice of b to move the P-matrix pole out of the vicinity of 750–800 MeV.

The S-wave states are expected to be more sensitive to the choice of b because there is less of a physical barrier (making $\partial s_0/\partial b$ greater). This may be seen in Figs. 8(b) and 8(c) where we have plotted $s_0(b)$ for the $\pi\pi$ $I=0$ and $I=2$ channels. Also

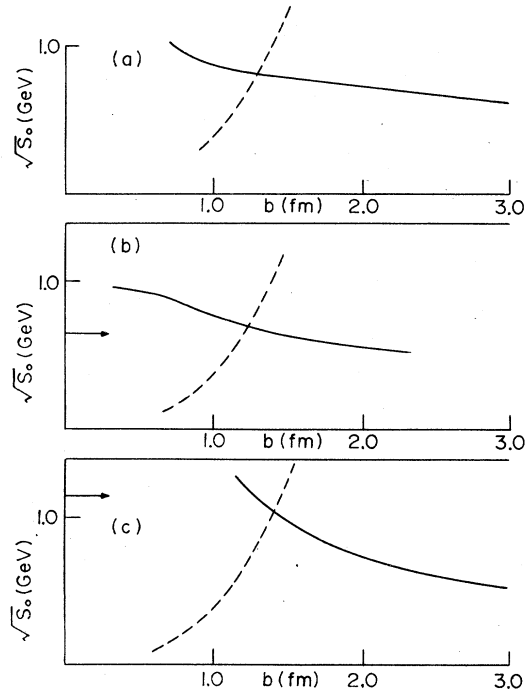

FIG. 8. b dependence of the P-matrix pole position for (a) the ρ-meson, (b) the lowest $\pi\pi^0$ S-wave primitive, (c) the $\pi\pi^2$ exotic S-wave primitive. The dashed curve indicates the $\sqrt{s_0}$ dependence of b estimated from the bag model. The arrows in (b) and (c) locate the predicted primitive masses in the bag model.

shown in Fig. 8 is the bag parametrization of b [Eq. (3.7)]. A nontrivial result of our analysis is that the intersection of the two curves in Figs. 8(b) and 8(c). which marks the mass of the primitive with the bag prescribed radius, also coincides with the mass of the primitive calculated in the model. The location of the $I=2$ primitive is particularly sensitive to b, indicating that this object is actually created by the imposed spherical boundary condition, and presumably has no nearby pole of the S matrix corresponding to it.

ACKNOWLEDGMENTS

The authors would like to thank their colleagues in the MIT theory group, particularly Professor DeTar, Professor Johnson, and Professor Kerman, for helpful discussions. They are also grateful to Dr. C. Rebbi for an enlightening conversation. This work was supported in part by the U. S. Department of Energy under Contract No. EY-76-C-02-3069.

APPENDIX A: HIGHER PARTIAL WAVES

We repeat the exercise of Sec. II leading to Eq. (2.3), except instead of the functions $e^{\pm ikr}$ we introduce the spherical Bessel functions $e_l^{\pm}(kr)$, defined to approach $e^{\pm i(kr+l\pi/2)}$ as $r\to\infty$, and instead of $\cos k(r-b)$ and $\sin k(r-b)/k$, $C_l(r,b)$ and $D_l(r,b)$ which satisfy the wave equation and are defined by the equations

$$C_l(b,b)=1, \quad D_l(b,b)=0, \qquad C_l'(b,b)=0, \quad D_l'(b,b)=1. \tag{A1}$$

For simplicity consider only one channel. The S_l matrix is defined by the asymptotic form of the wave function:

$$\psi_l(r)=A[e_l^-(kr)-\delta_l e_l^+(kr)], \quad r>b \tag{A2}$$

whereas the matching functions C_l and D_l define the P_l matrix:

$$\psi_l(r)=B[C_l(r,b)+P_l D_l(r,b)]. \tag{A3}$$

Here A and B are normalization constants. Using Eqs. (A1)–(A3), we easily find

$$P_l=\frac{d}{dr}\frac{e_l^-(kr)-S_l e_l^+(kr)}{e_l^-(kb)-S_l e_l^+(kb)}\bigg|_{r=b}. \tag{A4}$$

If we define a dimensionless P matrix in units of $1/b$, and call $x=bk$, we find

$$\frac{P_l}{x}=\frac{e_l^{-\prime}(x)-S_l e_l^{+\prime}(x)}{e_l^-(x)-S_l e_l^+(x)}. \tag{A5}$$

Our old S-wave result is easily obtained:

$$\frac{P_0}{x}=\frac{-ie^{-ix}-iS_0e^{ix}}{e^{-ix}-S_0e^{ix}}=\cot[\delta_0(x)+x]. \tag{A6}$$

The P wave is more involved. We give it here for easy reference:

$$e_1^{\pm}(x)=\pm ie^{\pm ix}(1\pm i/x), \tag{A7}$$

and (A5) becomes, after some algebra,

$$P_1=-(1+x^3\tan\phi)/(1+x^2)$$

with (A8)

$$\phi\equiv\delta_1(x)+x+\tan^{-1}(1/x).$$

Finally, we note that Eq. (A5) generalizes to the multichannel case:

$$P_l=[e_l^{-\prime}(kb)-e_l^{+\prime}(kb)\tilde{S}_l]/[e_l^-(kb)-e_l^+(kb)\tilde{S}_l]^{-1}, \tag{A9}$$

where

$$\tilde{S}_l=\frac{1}{\sqrt{k}}S_l\sqrt{k},$$

and that $P=1/R$ (where R is the Wigner-Eisenbud matrix) for all l.

APPENDIX B: FINAL-STATE INTERACTIONS

We show in this appendix, for S-wave potential scattering, how the P matrix can be introduced

at a value of r where there is still a residual interaction.

For $r > b$, we define

$$\psi(r) = C(r,b) + PD(r,b)\,, \tag{B1}$$

where, as usual, C and D satisfy the correct wave equation for $r > b$ and the boundary conditions

$$C(b,b) = 1, \quad D(b,b) = 0\,, \qquad C'(b,b) = 0, \quad D'(b,b) = 1\,. \tag{B2}$$

Thus, ψ satisfies the integral equation

$$\psi(r) = \cos k(r-b) + \frac{P}{k}\sin k(r-b) + \frac{1}{k}\int_b^r dr'\,\sin k(r-r')\,V(r')\psi(r')\,. \tag{B3}$$

Assuming the solution ψ of Eq. (B3) to be known, we go to asymptotic r and find

$$\psi(r) \sim \tfrac{1}{2}e^{ik(r-b)}(1 - iP/k) - \frac{ie^{ikr}}{2k}\int_b^\infty dr'\,e^{-ikr'}\,V(r')\psi(r') + \text{c.c.}\,, \tag{B4}$$

from which

$$S = -e^{-2ikb}\,\frac{1 - iP/k - (i/k)\int_b^\infty e^{-ik(r'-b)}\,V(r')\psi(r')\,dr'}{1 + iP/k + (i/k)\int_b^\infty e^{ik(r'-b)}\,V(r')\psi(r')\,dr'} \tag{B5}$$

or

$$S = -e^{-2ikb}\,\frac{1 - i\bar{P}/k}{1 + i\bar{P}/k}, \tag{B6}$$

with

$$\bar{P} = \frac{P + \int_b^\infty dr'\,\cos k(r'-b)[C(r',b) + PD(r',b)]\,V(r')}{1 - (1/k)\int_b^\infty dr'\,\sin k(r'-b)[C(r',b) + PD(r',b)]\,V(r')}\,. \tag{B7}$$

Provided the integrals in (B7) are all small, the poles and residue of P and $\bar{P}$ will be very close. We may estimate the effect by setting

$$C(r',b) \sim \cos k(r'-b), \quad D(r',b) \sim [\sin k(r'-b)]/k$$

and substituting these functions into (B7). We find for $\bar{P}$ (in units of $1/b$)

$$\bar{P} = \frac{P[1 + (1/2k)\int_b^\infty dr'\,\sin 2k(r'-b)\,V(r')] + \int_b^\infty dr'\,\cos^2 k(r'-b)\,V(r')b}{1 - (1/2k)\int_b^\infty dr'\,\sin 2k(r'-b)\,V(r') - (P/k)\int_b^\infty dr'\,\sin^2 k(r'-b)\,V(r')} \tag{B8}$$

$$= \frac{P(1 + I_2) + I_1}{1 - I_2 - PI_3}\,. \tag{B9}$$

Let $V \sim k_0^2 e^{-Mr}$; then at $k = 0$ (the worst point for a monotonic potential) the relevant integrals are, respectively,

$$I_1 = \frac{k_0^2 b}{M}e^{-Mb}, \quad I_2 = \frac{k_0^2}{M^2}e^{-Mb}, \qquad \text{and} \qquad I_3 = \frac{k_0^2}{bM^3}e^{-Mb}\,. \tag{B10}$$

If $M \sim M_\rho$, then $Mb \gg 1$, and the first integral is the most dangerous. However, I_1 is only involved in the residue of the pole in $\bar{P}$. The shift in pole location is proportional to I_3. Now for ρ exchange between pions

$$k_0^2 \simeq \frac{g^2}{4\pi}\,\frac{8k^2 + 4m_\pi^2 + m_\rho^2}{W}\,\frac{1}{b}\,(2\mathcal{P}_0 - \mathcal{P}_2)\,, \tag{B11}$$

where

$$\Gamma_\rho \simeq \frac{1}{3}\,\frac{g^2}{4\pi}\,\frac{P_\pi^3}{w_\pi^2} \quad (w_\pi = m_\rho/2)\,,$$

and $\mathcal{P}_0$ projects on $I = 0$, $\mathcal{P}_2$ on $I = 2$. We have, then, with $g^2/4\pi \simeq 1$, from (B10) and (B11), for $I = 0$ and $W \sim 650$ MeV,

$$I_1 \sim 6e^{-m_\rho b} \sim 0.05$$

for $I = 0$, whereas for $I = 2$, and $W \sim 1$ GeV

$$I_1 \sim 0.03.$$

The residues of our model are then modified by ~3–5%. The pole shifts are down by $(1/m_\rho b)^2 \sim 1/25$ and therefore totally negligible.

[1]T. A. DeGrand, R. L. Jaffe, K. Johnson, and J. Kiskis, Phys. Rev. D 12, 2060 (1975).
[2]R. L. Jaffe, Phys. Rev. D 15, 267, 281 (1977).
[3]Consider, for example, the S-wave configuration $[(Q_1\bar{Q}_2)^8(Q_3\bar{Q}_4)^8]^1$. A change of coupling transformation will display the color-singlet subunits, here $\{(Q_1\bar{Q}_4)^1(Q_3\bar{Q}_2)^1\}^1$, which are present.
[4]The approximation is not an intrinsic limitation of the bag model, which can permit color-singlet separation both by admixture of higher configurations and by distorting the bag boundary from its spherical shape, as shown by DeTar in his study of the two-nucleon problem [C. DeTar, Phys. Rev. D 17, 302 (1978); 17, 323 (1978)]. Unfortunately, DeTar's program has the problem that while a "potential energy" $V(r)$ can be calculated, it is not obvious into what Schroedinger equation $V(r)$ must be inserted.
[5]Particle Data Group, Phys. Lett. 75B, 1 (1978).
[6]The wiggles are a consequence of the sharp boundary of the square well. For a smoothed out potential the phase shift decreases monotonically to zero.
[7]E. P. Wigner and L. Eisenbud, Phys. Rev. 72, 29 (1947); G. Breit and W. G. Bouricius, *ibid.* 75, 1029 (1949); H. Feshbach and E. L. Lomon, Ann. Phys. (N.Y.) 29, 19 (1964).
[8]Note that the center of mass, r_c, is not fixed in the rigid-cavity treatment of the bag model. Therefore, the "mass" calculated in this approximation appears to include a kinetic energy of center-of-mass motion. This problem has been discussed recently in the study of solitons. In the bag model, Rebbi found (Ref. 9) that this effect reduces the actual mass by a factor proportional to $1/R$. But the phenomenological fits of Refs. 1 and 2 already include a term in $M(R)$ proportional to $1/R$ with negative coefficient adjusted to fit known masses. Therefore, the effect of center-of-mass motion has already been removed from the cavity spectrum.
[9]C. Rebbi, Phys. Rev. D 12, 2407 (1975).
[10]This is not a decomposition on a physical Hilbert space. Physical states such as $\vec{\pi}$—a color octet meson with the flavor quantum number of the pion—do not even exist. Instead Eq. (3.8) represents a decomposition of the multiparticle S-wave wave function onto a basis of S-wave $Q\bar{Q}$ states with the flavor, spin, and color quantum numbers as labeled. Thus $|\vec{\omega}\cdot\vec{\omega}\rangle$ is a color-singlet $Q^2\bar{Q}^2$ state in which each $Q\bar{Q}$ pair has the quantum numbers of a color-octet ω meson. We will interpret the coefficients in this expansion as indicative of the actual coupling of the four-quark system to meson-meson channels.
[11]We have not made a systematic error analysis for these fits, nor have we attempted to resolve conflicts between experiments. Our calculations were made with data at hand and should be regarded as illustrative. The parameters quoted in Table I will no doubt be revised when a more systematic analysis of the data is made.
[12]H. Becker *et al.* (CERN-Munich Collaboration), paper submitted to the XIX International Conference on High Energy Physics, Tokyo, 1978 (unpublished).
[13]G. Gruyer *et al.*, Nucl. Phys. B75, 189 (1974).
[14]M. J. Corden *et al.*, Rutherford Laboratory Report No. RL-78-067, 1978 (unpublished).
[15]P. Estabrooks, Carleton University report, 1978 (unpublished).
[16]It is interesting that for small values of $\xi_{K\bar{K}}$ the pole in the reduced P matrix is near $K\bar{K}$ threshold. Thus, the association of the rapid phase variation in δ_0^0 with $K\bar{K}$ threshold may be no accident.
[17]A. D. Martin, in *Phenomenology of Quantum Chromodynamics*, proceedings of the XIII Rencontre de Morcond, 1978, edited by J. Trân Thanh Vân (Edition Frontières, Dreux, France, 1978), p. 363.
[18]In order to simplify the calculation, the density (r) was actually calculated using a constant single-quark density rather than bag-model wave functions. Since the radial dependence in $\rho(r)$ is mainly geometrical, this approximation will not change the answer appreciably. The mean square radius used in Eq. (3.5) was calculated with actual bag-model densities, however.
[19]W. Hoogland *et al.*, Nucl. Phys. B126, 109 (1977).
[20]P. Estabrooks *et al.*, Nucl. Phys. B133, 490 (1978).
[21]S. D. Protopopescu *et al.*, Phys. Rev. D 7, 1279 (1973).